MONITORING OATS AND WINTER WHEAT WITHIN-FIELD SPATIAL VARIABILITY BY SATELLITE IMAGES*

J. Kumhálová[1], P. Novák[1], M. Madaras[2]

[1]Czech University of Life Sciences Prague, Prague, Czech Republic
[2]Crop Research Institute, Prague, Czech Republic

Remote sensing is a methodology using different tools to monitor and predict yields. Spatial variability of crops can be monitored through sampling of vegetation indices derived from the entire crop growth; spatial variability can be used to plan further agronomic management. This paper evaluates the suitability of vegetation indices derived from satellite Landsat and EO-1 data that compare yield, topography wetness index, solar radiation, and meteorological data over a relatively small field (11.5 ha). Time series images were selected from 2006, 2010, and 2014, when oat was grown, and from 2005, 2011 and 2013, when winter wheat was grown. The images were selected from the entire growing season of the crops. An advantage of this method is the availability of these images and their easy application in deriving vegetation indices. It was confirmed that Landsat and EO-1 images in combination with meteorological data are useful for yield component prediction. Spatial resolution of 30 m was sufficient to evaluate a field of 11.5 ha.

vegetation indices, plant variability, yield, topography, phenology, crop monitoring

DE GRUYTER OPEN

doi: 10.2478/sab-2018-0018
Received for publication on September 22, 2017
Accepted for publication on November 29, 2017

INTRODUCTION

Crop yield is a result of different occurrences during the entire plant growth process and can also be dependent on crop growth variability. Begue et al. (2008) noted that crop growth variability is related to multiple factors that can be time-independent (i.e. topography, soil type and depth) or time-dependent. Annually linked factors may include anomalies in planting, emergence, or weather conditions. Seasonally linked factors can include plant diseases, weed development, severe climatic events or irrigation system malfunctions. These time-independent and time-variable factors can also interact, leading to complex spatiotemporal crop vigour patterns (Machado et al., 2002).

Topography was an obvious cause of variation in field crops (Godwin, Miller, 2003) and water is the most limiting factor in agriculture. The spatial distribution of water on a field is influenced by lateral flow and is thus controlled in part by differences in elevation. Schmidt, Persson (2003) examined three methods of deriving potential flow accumulation from digital elevation models (DEM). Their results indicated that the topographic wetness index (TWI) can be used to assess the potential soil moisture pattern on a field and changes in soil texture caused by erosion processes.

Solar energy is an important fundamental to photosynthesis and evapotranspiration (Woodwell, 1967), and crop growth models (Hansen, 1999). Only solar radiation in the 0.4–0.7 μm wavelength interval supports photosynthesis in green plants. This spectral region is referred to as photosynthetically active radiation (PAR) (Daughtry et al., 1992).

Numerous methods can be used to monitor yield variability and topographic impact on yield, including ground-based sampling, tractor-mounted sampling, remote sensing from helicopters and aircraft, and

* Supported by the Ministry of Agriculture of the Czech Republic, Projects No. MZe RO0417 and No. QJ1520028.

satellite remote sensing (Jones, Vaughan, 2010). Satellite remote sensing systems not only cover large surface areas but can also repeatedly view the same target area. Existing literature refers to monitoring the spatial variability of yields via Landsat images for crops in different scenarios, such as cotton yields in a 50-ha field (Guo et al., 2012), maize and soybeans in a 100 × 50 km area (Doraiswamy et al., 2004) and different species in two Landsat scenes (Julien et al., 2011).

Spectral vegetation indices have been widely shown to vary not only with the seasonal variability of green foliage but also across space, thus making them suitable for detecting within-field spatial variability. Jamali et al. (2015) noted that the temporal trend analysis of the Normalised Difference Vegetation Index (NDVI) was particularly useful in monitoring and characterising the response of land cover to phenomena with time scales ranging from seasonal variabilities of plant phenology caused by changes in temperature and rainfall regimes (Heumann et al., 2007) to gradual inter-annual climate changes (Jacquin et al., 2010). Less frequently mentioned vegetation indices in existing literature include the Green Normalised Vegetation Index (GNDVI) (Nigon et al., 2014), the Moisture Stress Index (MSI) (Dupigny-Giroux, Lewis, 1999), the Chlorophyll Vegetation Index (CVI) (Vincini et al., 2008), and the Optimised Soil Adjusted Vegetation Index (OSAVI) (Haboudane et al., 2002).

The major goal of this study is to discuss the possibilities of evaluating yield variability with the aid of selected vegetation indices (VI) computed during the growth of winter wheat (2005, 2011, 2013) and oats (2006, 2010, 2014). The study also seeks to evaluate the relationships between VI, TWI, yield, and the meteorological data (precipitation, temperature, global solar radiation, and PAR) obtained for the given growth stages.

MATERIAL AND METHODS

Experimental data for this study were obtained from an 11.5-ha experimental field in Prague-Ruzyne (50°05′N; 14°17′30″E), the Czech Republic. Most of the field has a southern aspect with an elevation ranging from 338.5 to 357.5 m a.s.l. and the average slope is 6%. The soil of this experimental plot can be classified as Haplic Luvisol. The average precipitation is 526 mm per year, and the average temperature is 7.9°C. Total monthly precipitation, temperature, global solar radiation (GSR) and PAR data for this area were provided by local agro meteorology station; the data are presented in Fig. 1a, b.

Conventional arable soil tillage technology based on 0.25 m ploughing and fixed crop rotation was applied in this field.

The yields of this field have been measured since 2003. A combine harvester equipped with

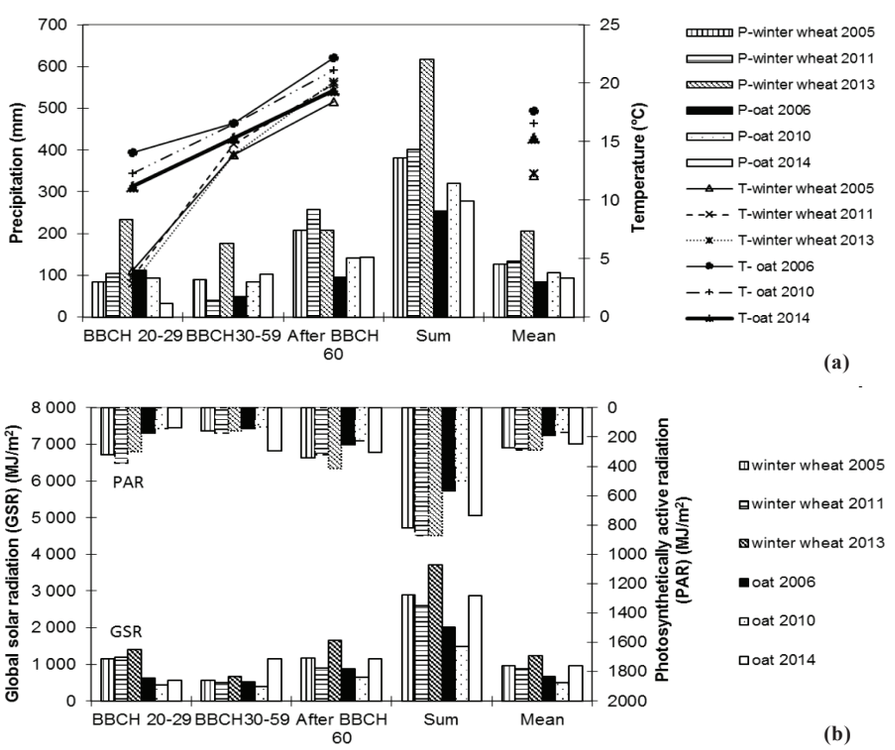

Fig. 1. Graphs of precipitations and temperatures (**a**), and global solar radiation and photosynthetically active radiation (**b**) at different growth stages by BBCH scale recorded in the experimental field for winter wheat in 2005, 2011, 2013, and for oat in 2006, 2010, and 2014

Table 1. Summary statistics and method of interpolation used for plant yield (t ha^{-1}) in selected years 2005 and 2011 (winter wheat), 2006, 2010, 2014 (oat)

	Oat yield			Winter wheat yield	
	2006	2010	2014	2005	2011
Count	8 822	9 024	10 129	8 236	7 548
Mean	4.219	2.254	4.414	6.081	7.053
Median	4.287	2.354	4.228	6.318	7.218
Mode	4.973	2.900	0.72	6.485	5.646
Sample variance	0.909	0.726	3.247	1.308	3.814
Standard deviation	0.953	0.852	1.802	1.143	1.953
Minimum	0.989	0.101	0.098	2.075	0.589
Maximum	7.224	4.825	8.994	9.929	13.458
Skewness	–0.515	–0.359	0.470	–0.806	–0.141
Method of interpolation	Kriging				
Method of estimation	Method of moments (MoM)				
Variogram model	Exponential				
Distance parameter (r)	23.4	26.0	12.3	32.5	45.3
Approximate range (3 × r)	70.2	78.0	36.9	97.5	135.9
Nugget variance	0.211	0.222	0.886	0.215	1.380
Sill variance	0.655	0.428	3.026	1.285	3.260

a LH 500 yield monitor (LH Agro, Denmark) and a DGPS (Differential Global Positioning System) receiver with EGNOS (European Geostationary Navigation Overlay Service) correction was used. The precision of the equipment was ± 0.1 to 0.3 m horizontally and ± 0.2 to 0.6 m vertically. Because of the large amount of data points for every year studied (more than 8000), the Method of Moments (MoM) was used to compute the experimental variograms. Weighted Least Squares approximation in GS+ (Gamma Design Software, St. Painwell, USA) was used. Only yield data from 2005, 2006, 2010, 2011 and 2014 were used (see Fig. 2); the 2013 yield data were not measured because of a sudden failure of the yield monitor. The summary

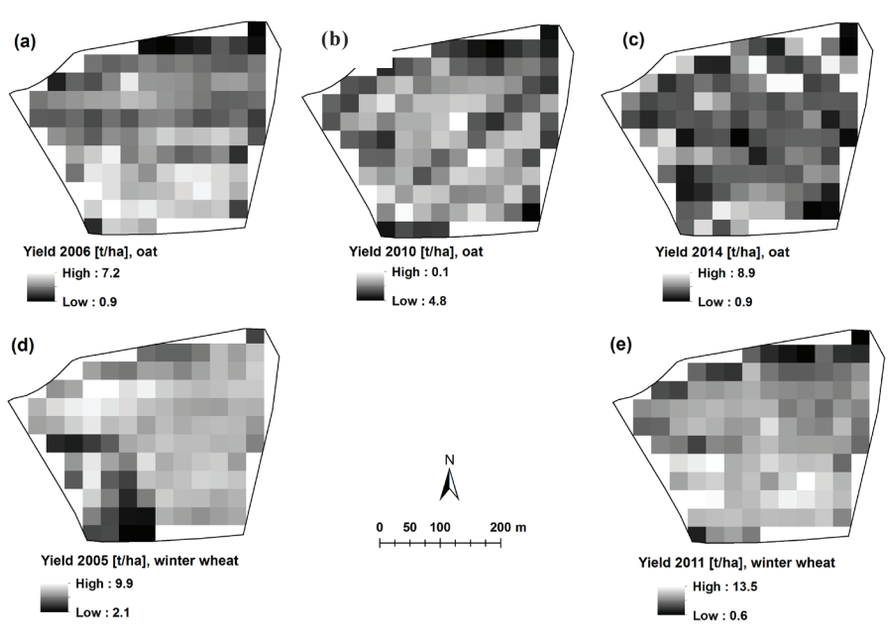

Fig. 2. Maps of krigged yield predictions in the experimental field during the observed years: 2006 – oats (**a**), 2010 – oats (**b**), 2014 – oats (**c**), 2005 – winter wheat (**d**), and 2011 – winter wheat (**e**).

Table 2. Available Landsat and EO-1 images of the study site for the selected terms

Image date	Type of satellite	Type of sensor	Image date	Type of satellite	Type of sensor
Winter wheat			Oat		
16/04/2005	Landsat 5	TM	13/06/2006	Landsat 5	TM
02/05/2005	Landsat 5	TM	22/05/2006	EO-1	ALI
03/06/2005	Landsat 5	TM	08/06/2010	Landsat 5	TM
04/06/2011	Landsat 7	ETM+	17/06/2010	Landsat 5	TM
19/05/2011	Landsat 7	ETM+	19/06/2014	Landsat 8	OLI
24/04/2011	Landsat 7	ETM+	28/06/2014	Landsat 8	OLI
26/05/2011	Landsat 7	ETM+			
15/05/2013	Landsat 8	OLI			
16/06/2013	Landsat 8	OLI			

statistics and methods of interpolation used for the estimation of crop yields in the selected years are shown in Table 1.

The topographic data were obtained by using LiDAR (Light Detection and Ranging) data graciously provided by the Czech Office for Surveying, Mapping and Cadastre. B r a z d i l (2012) guaranteed an average error of elevation as determined by the digital terrain model of the Czech Republic 4th generation (DTM 4G) of 0.13 m on arable land without vegetation; this was the case for our experimental field.

Elevation data were interpolated by inverse distance weighting (IDW) as an alternative to kriging in ArcGIS 10.3.1 to create a digital elevation model (DEM). The detailed description of the interpolation has been reported by K u m h a l o v a et al. (2011). A slope model (SM) and a flow accumulation model (FAM) were then derived from the DEM-D8 algorithm. K u m h a l o v a et al. (2014) noted that TWI can be a good alternative to FAM from D8 or MFD8 algorithm. TWI was therefore used to describe water distribution on the field. TWI uses SM and FAM raster data as inputs, based on the concept that low-gradient areas will gather water (high TWI values), whereas steep convex areas will shed water (low TWI values). TWI values are non-dimensional relative indices and vary by landscape type and DEM (see Fig. 3a). All topography models were created in ArcGIS 10.3.1 software.

Global solar radiation (GSR) was calculated with the help of the solar radiation analysis tool of the ArcGIS software. DEM calculated from the LiDAR data were selected as the input raster. The intervals from BBCH 20 to the date of image acquisition were selected for multi-day configurations. The resulting rasters from all periods were spatially very similar and varied only fractionally by the value of radiation in WH m^{-2}. The GSR raster from BBCH 20 to BBCH 37 (the date of image acquisition April 4, 2011) was used for visualisation purposes only (see Fig. 3b).

For this study, a set of fifteen cloud-free images (14 Landsat images and one EO-1 image) were provided by the USGS (http://glovis.usgs.gov) (Table 2). The images were acquired at a 30-m resolution.

The Fast Line-of-Sight Atmospheric Analysis of Hypercubes was used for atmospheric correction (e.g., L i et al. 2014). All image pre-processing was implemented with ENVI software (version 5.1; Excelis, Inc., McLean, USA).

The selected vegetation indices (CVI, GNDVI, MSI, NDVI, and OSAVI) were computed for every image with ENVI software. Table 3 shows a summary of the indices evaluated in this study. All images were then exported into ArcGIS software. The yield, TWI and solar radiation raster datasets were resampled by changing the cell size according to satellite image outputs to 30 m. There were only 110 pixels on the 11.5-ha experimental field area after the resampling process. All rasters were processed by using the Extract Multi Values to Point Tool (Spatial Analyst Tool, ArcGIS software, version 10.3.1; ESRI, Redlands, USA). This tool extracts cell values at locations specified in a point feature class from one or more rasters and records the values to the attribute table of the point feature class. Data from the attribute table were then exported to STATISTICA 12 software (StatSoft Inc., Tulsa, USA) for data analysis.

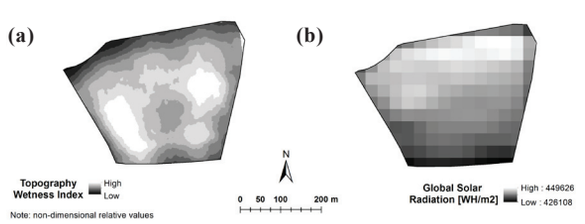

Fig. 3. Topography Wetness Index model map in the experimental field (**a**) and Global Solar Radiation from the period from BBCH 20 to June 4, 2011 (the date of image acquisition) (**b**)

Table 3. Summary of the indices evaluated in this study

Index	Name	Formula	Developed for	Developed by
CVI	Chlorophyll Vegetation Index	$= R_{NIR} \times \frac{R_R}{R_{G^2}}$	leaf chlorophyll content	Vincini et al. (2008)
GNDVI	Green normalised vegetation index	$= (R_{NIR} - R_G)/(R_{NIR} + R_G)$	chlorophyll	Gitelson et al. (1996)
MSI	Moisture stress index	$= \frac{R_{MidIR}}{R_{NIR}}$	leaf water content	Rock et al. (1985)
NDVI	Normalised difference vegetation index	$= (R_{NIR} - R_R)/(R_{NIR} + R_R)$	structure	Rouse et al. (1974)
OSAVI	Optimized Soil Adjusted Vegetation Index	$= (1 + 0.16) \times \frac{R_{NIR} - R_R}{R_{NIR} + R_R + 0.16}$	canopy structure with soil influence	Rondeaux et al. (1996)

R_G, R_{NIR}, R_{MidIR}, R_R are the reflectances for green, red, middle IR and NIR bands, respectively

RESULTS

Correlation matrices between the yield, TWI, global solar radiation, and vegetation indices in the given terms and years are shown in Table 4.

Oat crops were monitored in 2006, 2010, and 2014. The mean yield value reached 4.219 t ha^{-1} in 2006 (Table 1). High average temperature (14.1°C) at the early developmental phases of the oat plants caused fast tilling and an early enclosure of the crops. This corresponds to higher values of vegetation indices OSAVI (0.906) and CVI (9.475). Precipitation in May secured an optimal water supply. This corresponds to a significantly low MSI index value on May 22, 2006 (0.042). Plants in this growing phase had optimal conditions for rapid development. However, due to warm and dry conditions, the first half of June caused a local increase in plant water stress, which corresponds to an increased MSI index (0.351) on June 13, 2006. Lack of precipitation in the period BBCH 30–59 caused an increase in plant water stress and thus increased the influence of topography on the yield. The concentration of higher yield values in the area of accumulative depressions (concave areas) is apparent in Fig. 3a.

Very low yields (2.254 t ha^{-1}) were measured in 2010 compared to other seasons (Table 1). This year was characterised by even rainfall distribution (Fig. 1a). A colder than normal spring decelerated the development of plants in their early phenological phases. Subsequent increases in temperature brought improvement. This corresponded to higher correlation values between NVDI and GNDVI indices and yield (0.481/0.520) in both monitored periods (Table 4). Conversely, the impact of topography was less significant due to the sufficient water supply. The MSI index in both monitored periods reached low values (0.268 and 0.254), and the GSR (1483.2 MJ m^{-2}) and PAR (501.2 MJ m^{-2}) values were the lowest of the entire monitored period. The entire season was influenced by short periods of sunshine, heavy clouds and higher precipitation levels; this negatively influenced yield values. The oat crops were fully enclosed in either of the later phenological phases (after BBCH 60). When compared to other seasons, the yield reduction was also caused by excess precipitation in the period after BBCH 60. Heavy rainfall during the ripening season caused crop lodging on some parts of the field and thus reduced yield. The impact of topography cannot be positively determined from the yield map shown in Fig. 2b.

The last monitored oat-growing season was 2014, in which the mean yield reached 4.414 t ha^{-1}. Data indicate a more significant impact of topography on yield components than in the previous years (Fig. 2c). The degree of tilling was low and number of plants per m^2 was lower than in previous years, particularly in convex field areas. This was caused by a lack of precipitation (Fig. 1a) in the early phenological phases (BBCH 20–29). The plants thrived during this period, as indicated by the vegetation index values, and this deficit was compensated in later phenological phases. The 2014 season also confirmed the positive influence of higher GSR (2881.4 MJ m^{-2}) and PAR (735.2 MJ m^{-2}) values. Sunny weather had slightly increased the MSI values (0.364 – June 28, 2014), but water stress did not reach a level that would negatively affect yield components.

Wheat crops were monitored in 2005, 2011, and 2013. The yield mean value reached 6.81 t ha^{-1} (Table 1) in 2005. Even rainfall distribution was registered through all phenological phases in 2005, although precipitation, in spite of the evenness, reached the lowest total amount (127.2 mm) for the three monitored seasons. Lower CVI values (5.057) and to a lesser extent NVDI (0.681) and GNDVI (0.673) values, can be attributed to a slight short-term drought at the end of April 2005. This corresponds to an increased MSI (0.464). The MSI values significantly decreased in later phases (0.294 – May 2, 2005; 0.166 – June 3, 2005)

Table 4. Correlation coefficients (*r*) between various remote sensing indices and oat yields, TWI and GSR

	Date	Yield	TWI	GSR	Date	Yield	TWI	GSR	Date	Yield	TWI	GSR
Year	**2006**				**2010**				**2014**			
Yield		1	0.497***	–0.432***		1	0.449***	–0.099		1	0.002	0.112
TWI		0.497***	1	–0.169		0.449***	1	–0.172		0.002	1	–0.170
NDVI	**22.5.**	0.637***	0.326***	0.056	**8.6.**	0.481***	0.430***	0.042	**19.6.**	0.014	0.366***	0.268**
	13.6.	0.665***	0.509***	–0.044	**17.6.**	0.520***	0.499***	–0.041	**28.6.**	0.173	0.529***	–0.128
GNDVI	**22.5.**	0.568***	0.282**	0.038	**8.6.**	0.453***	0.421***	0.018	**19.6.**	0.028	0.305**	0.349***
	13.6.	0.672***	0.503***	–0.035	**17.6.**	0.555***	0.503***	–0.112	**28.6.**	0.190*	0.496***	–0.090
MSI	**22.5.**	0.421***	0.441***	–0.015	**8.6.**	–0.468***	–0.475***	0.032	**19.6.**	–0.062	–0.587***	–0.035
	13.6.	–0.627***	–0.515***	0.034	**17.6.**	–0.463***	–0.503***	0.078	**28.6.**	–0.132	–0.639***	0.207*
CVI	**22.5.**	0.296**	0.113	0.303**	**8.6.**	0.117	0.121	–0.077	**19.6.**	0.124	0.129	0.519***
	13.6.	0.375***	0.277**	–0.030	**17.6.**	0.347***	0.242*	–0.226*	**28.6.**	0.196*	0.430***	–0.050
OSAVI	**22.5.**	0.595***	0.304**	–0.012	**8.6.**	0.481***	0.430***	0.042	**19.6.**	0.014	0.366***	0.268**
	13.6.	0.665***	0.509***	–0.044	**17.6.**	0.520***	0.499***	–0.041	**28.6.**	0.173	0.529***	–0.128
Year	**2005**				**2011**				**2013**			
Yield		1	0.107	0.367***		1	0.579***	–0.380**		–	–	
TWI		0.107	1	–0.162		0.579***	1	–0.162		1	0.003	
NDVI	**16.4.**	0.543***	0.263**	0.182	**24.4.**	0.506***	0.336***	0.118	**15.5.**	0.406***	–0.004	
	2.5.	0.606***	0.130	0.559***	**19.5.**	0.760***	0.481***	–0.457***	**16.6.**	0.371***	–0.211*	
	3.6.	0.619***	0.376***	–0.005	**26.5.**	0.840***	0.570***	–0.569***				
					4.6.	0.724***	0.446***	–0.737***				
GNDVI	**16.4.**	0.480***	0.295**	0.212*	**24.4.**	0.522***	0.369***	0.147	**15.5.**	0.410***	0.000	
	2.5.	0.519***	0.123	0.505***	**19.5.**	0.741***	0.487***	–0.370***	**16.6.**	0.356***	–0.273**	
	3.6.	0.699***	0.292**	0.223*	**26.5.**	0.774***	0.560***	–0.521***				
					4.6.	0.692***	0.403***	–0.767***				
MSI	**16.4.**	–0.448***	–0.058	–0.537***	**24.4.**	–0.093	–0.107	–0.419***	**15.5.**	–0.425***	–0.006	
	2.5.	–0.591***	–0.126	–0.559***	**19.5.**	–0.684***	–0.522***	0.285**	**16.6.**	–0.470***	0.085	
	3.6.	–0.707***	–0.365***	–0.208*	**26.5.**	–0.792***	–0.619***	0.430***				
					4.6.	–0.785***	–0.533***	0.631***				
CVI	**16.4.**	0.239*	0.168	0.167	**24.4.**	0.288**	0.229*	0.117	**15.5.**	–0.074	0.288**	
	2.5.	0.219*	0.051	0.252**	**19.5.**	0.508***	0.351***	–0.236*	**16.6.**	0.290**	–0.446***	
	3.6.	0.399***	0.013	0.396***	**26.5.**	0.392***	0.375***	–0.287**				
					4.6.	0.562***	0.267**	–0.708***				
OSAVI	**16.4.**	0.544***	0.263**	0.182	**24.4.**	0.506***	0.336***	0.118	**15.5.**	0.406***	–0.004	
	2.5.	0.606***	0.129	0.559***	**19.5.**	0.761***	0.482***	–0.457***	**16.6.**	0.371***	–0.211*	
	3.6.	0.619***	0.376***	–0.005	**26.5.**	0.839***	0.570***	–0.569***				
					4.6.	0.724***	0.446***	–0.737***				

GSR = Global solar radiation, TWI = Topography wetness index, NDVI = Normalised difference vegetation index, GNDVI = Green NDVI, MSI = Moisture stress index, CVI = Chlorophyll vegetation index, OSAVI = Optimized soil adjusted vegetation index

levels of statistical significance: **P* < 0.05; ***P* < 0.01; ****P* < 0.001

and later phenological phases (after BBCH 60) when the wheat crops were well and evenly supplied by water. The yield in individual parts of the field was less influenced by topography (Fig. 2d) than in 2011 (Fig. 2e).

The yield mean value reached 7.053 t ha^{-1} in 2011. The impact of terrain topography on yield was greater than in 2005 due to deficient precipitation in the BBCH 30–59 growing phase. Tillering was reduced and slowed during spring; this corresponds to the OSAVI index

value (0.872 – April 24, 2011), particularly in the early monitored terms. The MSI index was also higher (0.364 – April 24, 2011). Stem elongation was due to a lack of precipitation, and this phase took longer than usual. The amount of precipitation in the period after BBCH 60 was the highest (257.4 mm) of the entire monitored period. This also explains the very low MSI values (0.229 – May 26, 2011; 0.123 – June 4, 2011) in later phases. However, there were clear high correlation values between the NDVI (0.724 – June 4, 2011) and GNDVI (0.692 – June 4, 2011) indices and the yield, which indicates proper water and nutrition supplies in later phenological phases (after BBCH 60 – see Table 4). The GSR (2609.6 MJ m^{-2}) and PAR (871.3 MJ m^{-2}) values were the lowest of the three monitored seasons of winter wheat crops (Fig. 1b). In particular, the ripening of wheat was slower than in the previous years. This also confirms the yield map shown in Fig. 2e.

The spatial yield pattern was not measured in 2013. A weighing of hauling means determined the yield mean to be 7.54 t ha^{-1}. This year was characterised by wet periods in spring and during the wheat ripening season. This was verified by high CVI values (12.095 – June 16, 2013). Plant growth was longer, and the plants still had high chlorophyll contents in the middle of June. The crops were well tillered and joined, as shown by the OSAVI values (1.094 – May 15, 2013; 1.026 – June 16, 2013). There was an apparent influence of high average temperature (20.1°C) and of the GSR and PAR values (Fig. 1) in later growing phases (after BBCH 60). In spite of high total precipitation, this caused a slight increase in MSI values (0.319 –June 16, 2013) in later periods when the top soil layers had locally dried. This increase, however, had no significant influence on the major yield components, which was verified by very high CVI values (6.598 – May 15, 2013; 12.095 – June 16, 2013).

DISCUSSION

Studies on crop within-field variability are based on different data sources, crops, and evaluation in existing literature. This study made on our experimental field showed that remote sensing tools can aid in determining the places that accumulate water and where plants are in the best condition all year round. Begue et al. (2008) found the same results in their research with sugarcane, and showed through an example using satellite remote sensing how cropping and environmental factors impact within-field temporal variability. Their results with sugarcane showed that it is necessary to determine crop phenology to correctly interpret the spatial pattern.

The use of satellite images can provide temporal information about the phenological state of the vegetation. Results indicated that a spatial resolution of 30 m for Landsat and EO-1 images is useful in determining temporal information on phenological states and plant conditions. Many studies have used Landsat images with a 30-m spatial resolution to evaluate different crops or landscape elements of different sizes. Chao Rodriguez et al. (2014) used Landsat image time series to study a small water body (11.5 ha) in Northern Spain and found that Landsat historical archives may still provide a wealth of environmental information. Landsat data has also been used by other authors on larger fields. Julien et al. (2011) used Landsat imagery for land use classification in a large agriculture area in Barrax (Spain); Guo et al. (2012) evaluated the spatial variability of cotton yields in a 50-ha field in relation to soil-apparent electrical conductivity, topography, and bare soil brightness based on remote sensing images (Landsat 5 TM) over multiple growing seasons.

Applications of vegetation indices have ranged from leaf to global levels. Most vegetation indices tend to be species specific and are thus not robust when applied across different species with different canopy architectures and leaf structures (Vina et al., 2011). In this research, we selected traditional vegetation indices that have been typically used in other studies to evaluate plant and yield variability. Most authors used either specific vegetation indices for selected problems, e.g. Nigon et al. (2014), or traditional vegetation indices for evaluating crop canopies.

We also found that it was necessary to have as many satellite images and vegetation indices as possible throughout the relevant phenological stages to properly estimate the yield components. This was also confirmed by Yang, Everitt (2002), who studied the dynamics of spectral vegetation indices to determine the best period to delineate potential yield zones.

Topography is one of the most important factors and can play a crucial role, particularly in dry years (Kumhalova et al., 2014). In the previous research (Kumhalova et al., 2011), the influence of topography on yield variability and the production potential of an experimental field were evaluated. We found that our results with small-grain crops corresponded well with those of other studies (Marques da Silva, Silva, 2008) using different crops under different climatic conditions. In addition, we discovered that the influence of topography on plant variability during the growing season can be estimated with the help of remote sensing tools. This was also confirmed by Guo et al. (2012), who reported that cotton yields had a stronger correlation with selected topography attributes in dry growing seasons than in wet growing seasons and that cotton yield variability patterns were relatively stable across different growing seasons. They used Landsat-5 TM images to evaluate crop yield variability and found that the NIR band may be the best choice for representing soil brightness when predicting crop yield variability. Their study showed

that remote sensing can be used for yield variability description.

CONCLUSION

The results presented in this article show a connection between the vegetation indices, phenophases, final yields, and TWIs that characterise topographic field conditions. The results showed that satellite images with a spatial resolution of 30 m were useful when evaluating an 11.5-ha field. The advantage of this processing method is an easy access to data inputs. Conversely, the disadvantage is a limited selection of images convenient for evaluation due to poor meteorological conditions during imagery.

Predicting the yield components based on analysing the growth state determined via remote sensing constitutes an interesting analysis tool. These analyses can be applied in advanced systems of precision agriculture and can serve as an element of managed agriculture, particularly on large land blocks or in agricultural services. In looking ahead, we can expect a further extension of growth imagery and an expansion of indexing to other field crops.

It will be necessary to determine other links between vegetation indices and crop parameters, as well as to further determine appropriate correlations between these parameters.

REFERENCES

Begue A, Todoroff P, Pater J (2008): Multi-time scale analysis of sugarcane within-field variability: improved crop diagnosis using satellite time series? Precision Agriculture, 9, 161–171. doi: 10.1007/s11119-008-9063-3.

Brazdil K (2012): Technical report to the digital terrain model of the 4th generation. http://geoportal.cuzk.cz/Dokumenty/TECHNICKA_ZPRAVA_DMR_4G_15012012.pdf. Accessed 19 November, 2014. (in Czech)

Chao Rodriguez Y, el Anjoumi A, Dominguez Gomez JA, Rodriguez Perez D, Rico E (2014): Using Landsat image time series to study a small water body in Northern Spain. Environmental Monitoring and Assessment, 186, 3511–3522. doi: 10.1007/s10661-014-3634-8.

Daughtry CST, Gallo KP, Goward SN, Prince SD, Kustas WP (1992): Spectral estimates of absorbed radiation and phytomass production in corn and soybean canopies. Remote Sensing of Environment, 39, 141–152.

Doraiswamy PC, Hatfield JL, Jackson TJ, Akhmedov B, Prueger J, Stern A (2004): Crop condition and yield simulations using Landsat and MODIS. Remote Sensing of Environment, 92, 548–559. doi: 10.1016/j.rse.2004.05.017.

Dupigny-Giroux LA, Lewis JE (1999): A moisture index for surface characterization over a semiarid area. Photogrammetric Engineering & Remote Sensing, 65, 937–945.

Gitelson AA, Kaufman Y, Merzlyak MN (1996): Use of green channel in remote sensing of global vegetation from EOS-MODIS. Remote Sensing of Environment, 58, 289–298. doi: 10.1016/S0034-4257(96)00072-7.

Godwin RJ, Miller PCH (2003): A review of the technologies for mapping within-field variability. Biosystems Engineering, 84, 393–407. doi: 10.1016/S1537-5110(02)00283-0.

Guo W, Maas SJ, Bronson KF (2012): Relationship between cotton yield and soil electrical conductivity, topography, and Landsat imagery. Precision Agriculture, 13, 678–692. doi: 10.1007/s11119-012-9277-2.

Haboudane D, Miller JR, Tremblay N, Zarco-Tejada PJ, Dextraze L (2002): Integrated narrow-band vegetation indices for prediction of crop chlorophyll content for application to precision agriculture. Remote Sensing of Environment, 81, 416–426. doi: 10.1016/S0034-4257(02)00 018-4.

Hansen JW (1999): Stochastic daily solar irradiance for biological modelling applications. Agricultural and Forest Meteorology, 94, 53–63.

Heumann BW, Seaquist JW, Eklundh L, Jonsson P (2007): AVHRR derived phenological change in the Sahel and Soudan, Africa, 1982–2005. Remote Sensing of Environment, 108, 385–392. doi: 10.1016/j.rse.2006.11.025.

Jacquin A, Shereen D, Lacombe JP (2010): Vegetation cover degradation assessment in Madagascar savanna based on trend analysis of MODIS NDVI time series. International Journal of Applied Earth Observation and Geoinformation, 12, S3–S10. doi: 10.1016/j.jag.2009.11.004.

Jamali S, Jonsson P, Eklundh L, Ardo J, Seaquist J (2015): Detecting changes in vegetation trends using time series segmentation. Remote Sensing of Environment, 156, 182–195. doi: 10.1016/j.rse.2014.09.010.

Jones HG, Vaughan RA (2010): Remote sensing of vegetation: Principles, techniques, and applications. Oxford University Press, Oxford, New York.

Julien Y, Sobrino JA, Jimenez-Munoz JC (2011): Land use classification from multitemporal Landsat imagery using the Yearly Land Cover Dynamics (YLCD) method. International Journal of Applied Earth Observation and Geoinformation, 13, 711–720. doi: 10.1016/j.jag.2011.05.008.

Kumhalova J, Kumhala F, Kroulik M, Matejkova S (2011): The impact of topography on soil properties and yield and the effects of weather conditions. Precision Agriculture 12, 813–830. doi: 10.1007/s11119-011-9221-x.

Kumhalova J, Zemek F, Novak P, Brovkina O, Mayerova M (2014): Use of Landsat images for yield evaluation within a small plot. Plant, Soil and Environment, 60, 501–506.

Li P, Jiang L, Feng Z (2014): Cross-comparison of vegetation indices derived from Landsat-7 enhanced thematic mapper plus (ETM+) and Landsat-8 operational land imager

(OLI) sensors. Remote Sensing, 6, 310–329. doi: 10.3390/rs6010310.

Machado S, Bynum ED, Archer TL, Lascano RJ, Wilson LT, Bordovsky J, Segarra E, Bronson K, Nesmith DM, Xu W (2002): Spatial and temporal variability of corn growth and grain yield: Implications for site-specific farming. Crop Sciences, 42, 1564–1576. doi: 10.2135/cropsci2002.1564.

Marques da Silva JR, Silva LL (2008): Evaluation of the relationship between maize yield spatial and temporal variability and different topographic attributes. Biosystems Engineering, 101, 183–190. doi: 10.1016/j.biosystemseng.2008.07.003.

Nigon TJ, Mulla DJ, Rosen CJ, Cohen Y, Alchanatis V, Rud R (2014): Evaluation of the nitrogen sufficiency index for use with high resolution, broadband aerial imagery in a commercial potato field. Precision Agriculture, 15, 202–226. doi: 10.1007/s11119-013-9333-6.

Rock BN, Williams DL, Vogelmann JE (1985): Field and airborne spectral characterization of suspected acid deposition damage in red spruce (*Picea rubens*) from Vermont. In: Proc. Symposium on Machine Processing of Remotely Sensed Data, West Lafayette, USA, 71–81.

Rondeaux G, Steven M, Baret F (1996): Optimization of soil-adjusted vegetation indices. Remote Sensing of Environment, 55, 95–107. doi: 10.1016/0034-4257(95)00186-7.

Rouse JW, Haas RH, Schell JA, Deering DW (1974): Monitoring vegetation systems in the Great Plains with ERTS. In: Freden S.C., Mercanti E.P., Becker M. (eds): Third Earth Resources Technology Satellite-1 Symposium. Vol. 1: Technical Presentations, NASA SP-351. National Aeronautics and Space Administration, Washington, DC, 309–317.

Schmidt F, Persson A (2003): Comparison of DEM data capture and topographic wetness indices. Precision Agriculture, 4, 179–192. doi: 10.1023/A:1024509322709.

Vina A, Gitelson AA, Nguy-Robertson AL, Peng Y (2011): Comparison of different vegetation indices for the remote assessment of green leaf area index of crops. Remote Sensing of Environment, 115, 3468–3478. doi: 10.1016/j.rse.2011.08.010.

Vincini M, Frazzi E, D'Alessio P (2008): A broad-band leaf chlorophyll vegetation index at the canopy scale. Precision Agriculture, 9, 303–319. doi: 10.1007/s11119-008-9075-z.

Vincini M, Frazzi E, D'Alessio P (2008): A broad-band leaf chlorophyll vegetation index at the canopy scale. Precision Agriculture, 9, 303–319. doi: 10.1007/s11119-008-9075-z.

Woodwell GM (1967): Radiation and the patterns of nature. Science, 156, 461–470. doi: 10.1126/science.156.3774.461.

Yang C, Everitt JH (2002): Relationships between yield monitor data and airborne multidate multispectral digital imagery for grain sorghum. Precision Agriculture, 3, 373–388. doi: 10.1023/A:1021544906167.129 129

Corresponding Author:

doc. Mgr. Jitka K u m h á l o v á , Ph.D., Czech University of Life Sciences Prague, Faculty of Engineering, Kamýcká 129, 165 00 Prague–Suchdol, Czech Republic, phone: +420 224 383 148, e-mail: kumhalova@tf.czu.cz